nature plants

BRIEF COMMUNICATION

PUBLISHED: 25 JANUARY 2016 | ARTICLE NUMBER: 15220 | DOI: 10.1038/NPLANTS.2015.220

In vivo stoichiometry of photorespiratory metabolism

Cyril Abadie[1], Edouard R. A. Boex-Fontvieille[2], Adam J. Carroll[1] and Guillaume Tcherkez[1]*

Photorespiration is a major light-dependent metabolic pathway that consumes oxygen and produces carbon dioxide. In the metabolic step responsible for carbon dioxide production, two molecules of glycine (equivalent to two molecules of O_2) are converted into one molecule of serine and one molecule of CO_2. Here, we use quantitative isotopic techniques to determine the stoichiometry of this reaction in sunflower leaves, and thereby the O_2/CO_2 stoichiometry of photorespiration. We find that the effective O_2/CO_2 stoichiometric coefficient at the leaf level is very close to 2 under normal photorespiratory conditions, in line with expectations, but increases slightly at high rates of photorespiration. The net metabolic impact of this imbalance is likely to be modest.

Photorespiration is the CO_2-evolving metabolic process that recycles the product of O_2 fixation by ribulose-1,5-bisphosphate carboxylase/oxygenase (Rubisco), 2-phosphoglycolate. Under usual gaseous conditions (current atmospheric CO_2 and O_2 mole fraction), between 25 and 35% of ribulose-1,5-bisphosphate molecules are oxygenated rather than carboxylated by Rubisco[1] thereby leading to a considerable production of CO_2[2]. At the global scale, photorespiration is believed to evolve up to 29 Gt CO_2 per year[3]. The step responsible for CO_2 production is catalysed by the Gly decarboxylase (GDC)/Ser hydroxymethyltransferase (SHMT) complex that converts two molecules of Gly to one molecule of Ser, CO_2 and ammonium (NH_4^+)[4] as represented by the following net reaction:

$$2\,\mathrm{Gly} + \mathrm{NAD}^+ \rightarrow \mathrm{Ser} + \mathrm{NH_4}^+ + \mathrm{CO_2} + \mathrm{NADH}$$

Thus, the stoichiometric coefficient of the net reaction is 2 moles of Gly consumed per mole of Ser evolved. However, undesirable uncertainty remains whether this coefficient translates directly to leaf gas exchange: while it is known that fixation of one O_2 leads to synthesis of one Gly, it is uncertain whether 100% of this Gly is converted to Ser by GDC/SHMT. In fact, this step is believed to be limiting[5], causing a progressive increase in cellular Gly-to-Ser ratio and Gly content[6]. Other reports suggest that the GDC/SHMT step is simply bypassed[7] but in gas exchange calculations, a coefficient of exactly 2 is used[8]. Taken as a whole, it seems that the stoichiometric coefficient of the GDC/SHMT step is close to, but could potentially deviate from, two. However, no study has precisely quantified photorespiratory recycling efficiency *in vivo*. Even subtle alterations in GDC/SHMT-catalysed Gly utilization may have pervading consequences at the cellular level, simply because a build-up in Gly and/or Ser would sequester nitrogen atoms and this would have to be compensated for by increased nitrogen assimilation. In C_3 leaves, the metabolic flux associated with photorespiration is up to 100 times larger than nitrate reduction[9]; therefore, even a very small imbalance in photorespiratory recycling may impact on the plant nitrogen budget.

To address this question, we performed a series of isotopic labelling experiments and metabolome kinetics in sunflower (*Helianthus annuus* L.) leaves under different gaseous (CO_2/O_2) conditions (illustrated in Supplementary Fig. 1). Since the deviation from the theoretical coefficient of 2 is probably very small and may be confounded by experimental noise, we used specific quantitative isotopic methods. We first measured the rate of Gly decarboxylation when leaves were fed with [^{13}C-1]Gly (10% ^{13}C in C-1) using isotope ratio mass spectrometry and isotopic mass balance (Fig. 1). There was a clear but plateauing increase in the decarboxylation rate (in μmol m^{-2} s^{-1}) of exogenously added Gly as photorespiration (oxygenation rate v_o) increased, showing stimulation and apparent saturation of GDC activity (Fig. 1a). This effect was mostly caused by the isotopic dilution of Gly. In fact, identical experiments carried out with [^{13}C-2]Gly (99% ^{13}C in C-2) and subsequent analysis by gas chromatography/time of flight mass spectrometry demonstrated a negative relationship between position-specific isotope enrichment (% ^{13}C) in Gly and Ser, and v_o (Fig. 1b), showing the progressive dilution of exogenously applied isotopic Gly by endogenous photorespiratory Gly. The isotope enrichment in Gly and Ser was tightly correlated, and this effect did not originate from undesirable ^{13}C-labelling in photosynthetically fixed carbon (Fig. 1b, inset). Rather, the turnover of the Ser pool was rapid enough to reflect the isotopic signature in Gly. The isotope enrichment in the carbon atom derived from Gly in C_1-containing compounds (methenyl tetrahydrofolate and *S*-adenosylmethionine) also decreased considerably (Fig. 1c) and the Gly-to-Ser ratio increased, suggesting that the GDC/SHMT complex did not convert all of the Gly molecules into Ser so that Gly accumulated (Fig. 1d). The ^{13}C-enrichment and the molar content in metabolites were used to infer absolute ^{13}C content and thus net Gly utilization (Fig. 1d, inset). Observed values of net utilization were always very small, showing minimal imbalance in Gly metabolism. The values were all negative (except at 0% O_2) and indicated a slightly non-quantitative Gly consumption. However, the uncertainty associated with these values was too large to compute a precise effective stoichiometric coefficient (O_2 fixed per CO_2 release).

The effect of oxygenation on nitrogen metabolism was then examined by labelling with [^{15}N]Gly (98% ^{15}N, under otherwise identical experimental conditions) and ^{15}N absolute measurements by quantitative ^{15}N-NMR (nuclear magnetic resonance) analyses, in addition to isotope enrichment (% ^{15}N) determination by mass spectrometry (Fig. 2). The % ^{15}N appeared to be always larger by about 20% than that in ^{13}C (Fig. 1c, inset) simply showing the labelling of endogenous Gly by the recycling of [^{15}N]ammonium evolved from exogenous [^{15}N]Gly. In all cases, Ser represented the largest ^{15}N proportion reflecting the relative abundance of this metabolite in sunflower leaves (Fig. 2a). However, the ^{15}N content in leaf Ser decreased, whereas that in both Gly and Gln increased, showing the increasing competition with endogenous [^{14}N]Gly as v_o increased. Other metabolites always represented less than 10% of total ^{15}N (Fig. 2b). The amide nitrogen atom in Gln and the

[1]Research School of Biology, ANU College of Medicine, Biology and Environment, Australian National University, Canberra ACT 0200, Australia. [2]Laboratoire BVpam, EA3061, Université de Lyon/Saint-Etienne, 23 rue du Docteur Michelon, 42000 Saint-Etienne, France. *e-mail: guillaume.tcherkez@anu.edu.au

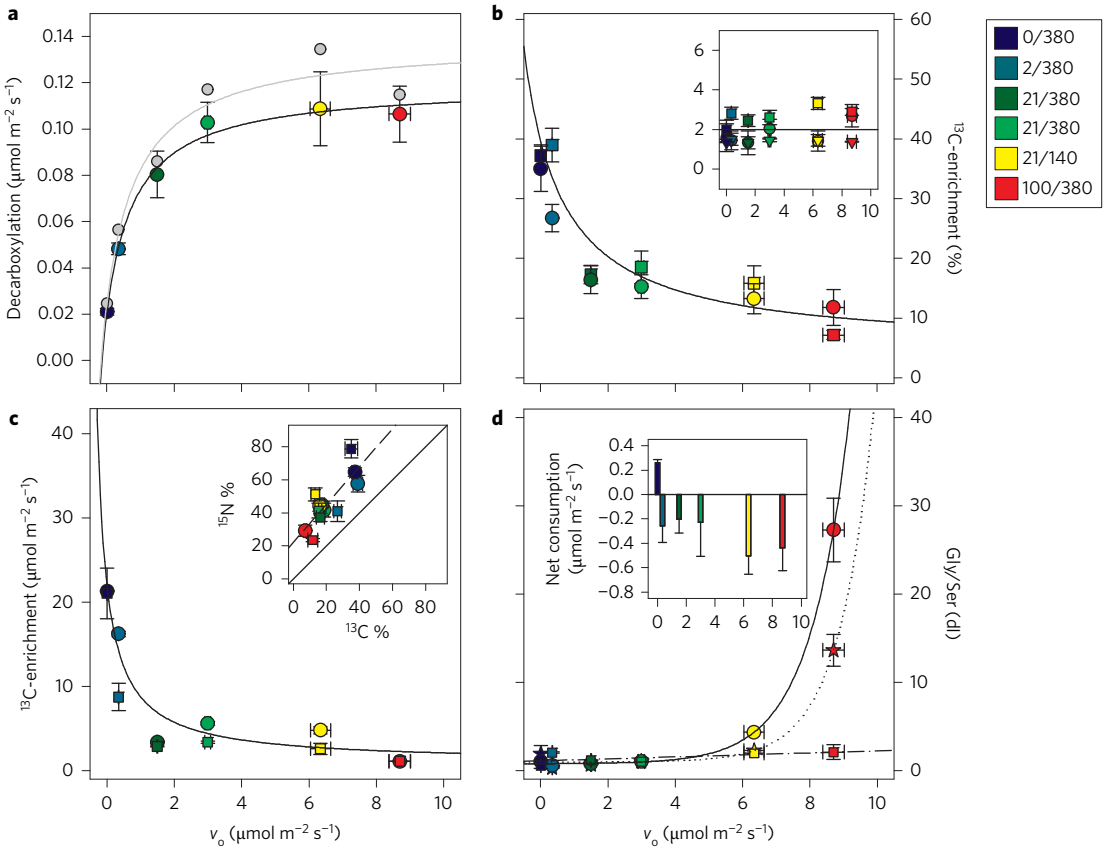

Figure 1 | Metabolite content and ^{13}C-enrichment on labelling with ^{13}C-Gly as a function of the oxygenation rate. a, Decarboxylation rate obtained with ^{13}C-1-Gly labelling. The rate corrected for refixation of decarboxylated $^{13}CO_2$ is shown in grey. **b**, Isotope enrichment (positional % in ^{13}C) in metabolites after labelling with ^{13}C-2-Gly: isotope composition in Gly (circles) and Ser (squares) (main plot), and in glycolate (circles), glycerate (squares) and fructose (triangles) (inset). **c**, Isotope enrichment (positional % in ^{13}C) in metabolites after labelling with ^{13}C-2-Gly: isotope composition in methylene-THF (circles) and SAM (squares) (main plot); relationship between the isotope enrichment (%) in ^{13}C and ^{15}N in Gly (circles) and Ser (squares) (inset). **d**, Gly (circles) and Ser (squares) content and Gly-to-Ser ratio (stars) expressed relative to 'usual' conditions (21% O_2, 380 µmol mol^{-1} CO_2) (main plot); net consumption of Gly (output minus input) calculated from ^{13}C enrichment and metabolite content (inset). Photorespiratory colour scale: O_2 (%)/CO_2 (µmol mol^{-1}). Lines represent trends to facilitate the reading. In the inset of **c**, the solid diagonal represents the 1:1 line. Each data point is the mean ± s.e. of three to seven measurements.

amine nitrogen atom in Gln + Glu represented the same ^{15}N content (Fig. 2c, inset), suggesting a higher average ^{15}N-labelling in amide than in amine groups and/or a heterogeneous ^{15}N partitioning among metabolites of the glutamine synthetase/glutamine oxoglutarate amino transferase (GS/GOGAT) cycle. ^{15}N absolute contents were then combined with isotope enrichment in ^{15}N to compute metabolic fluxes (Fig. 2c). All of the metabolic fluxes associated with photorespiration increased with v_o and the GDC/SHMT activity was always approximately one half of v_o. However, Gly consumption was slightly slower than Gly synthesis and the magnitude of this difference increased as v_o increased, reaching about 9% of v_o (0.84 µmol m^{-2} s^{-1}) in 100% O_2 (Fig. 2c). The computed effective stoichiometric coefficient (O_2 fixed per CO_2 release) was very close to 2, except at relatively large photorespiration rates (Table 1 and Supplementary Fig. 2). The impact of oxygenation on metabolic pools was further assessed using (1) metabolome kinetics when gaseous conditions were changed from normal (21% O_2, 380 µmol mol^{-1} CO_2) to low, normal or high photorespiratory conditions; (2) computation of apparent fluxes from metabolomics data and metabotype comparisons (Supplementary Figs 3–9). These data were also consistent with oxygenation activity nearly perfectly matching but slightly exceeding photorespiratory recycling capacity, thus leading to Gly accumulation at high photorespiration rates (see Supplementary Text).

This study provides compelling evidence that the ratio between oxygenation and photorespiratory CO_2 evolution is nearly perfectly 2, as is assumed by commonly used gas exchange models[1]. A slight stoichiometric imbalance may occur at high photorespiration so that a small fraction of Gly accumulates, thereby sequestering nitrogen atoms. This must be compensated for by a larger involvement of Glu (compared with Ser) as an amino donor for 2-phosphoglycolate conversion to Gly: in fact, the ^{15}N distribution found here appeared to be consistent with an increased consumption of Glu at large oxygenation rates (Fig. 2d). These effects explain the well-known Gly accumulation in illuminated leaves[6,10] and the enigmatic stimulating effect of photorespiration on 2-oxoglurate metabolism[11], day respiration[12] and nitrogen assimilation[9,13,14]. Here, experiments were carried out in the photosynthetic steady state under controlled conditions. In nature, where the CO_2 mole fraction and light vary and plants experience day–night cycles, the net overall effect of the small photorespiratory imbalance on leaf metabolites and nitrogen nutrition is likely to be modest.

Methods

Plant material, growth conditions and sampling. A horticultural variety of sunflower was used (*H. annuus* var. Sunrich). Sampling was made by instant freezing by liquid nitrogen spraying of the whole leaf (isotopic labelling) or using a punch (0.8 cm²) through a very small incision made on the chamber wall (metabolome kinetics). In the latter case, four samplings were done on the same leaf. The chamber wall was resealed after each sampling. As usual with gas exchange, there was slight overpressure in the system so that external air could not contaminate the atmosphere around the leaf during sampling (which took less than 10 s).

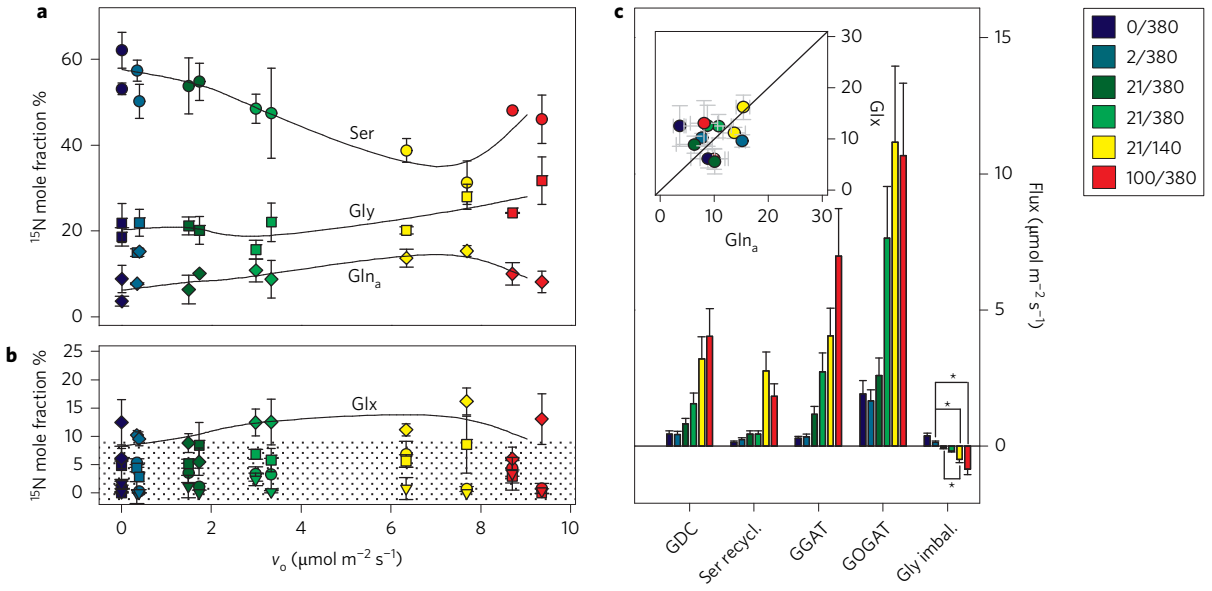

Figure 2 | ^{15}N-enrichment pattern and apparent fluxes on labelling with ^{15}N-Gly. a, Molar distribution of leaf ^{15}N between Ser (circles), Gly (squares) and the amide nitrogen atom of Gln (diamonds). **b**, The amine nitrogen atom of Gln and Glu (diamonds) and other metabolites: Ala (circles), Asx (squares) and ammonium (triangles). **c**, Relationship between the ^{15}N content in amide and amine nitrogen atoms of Gln and/or Glu (inset); reaction fluxes computed from molar ^{15}N distribution and isotope composition (% ^{15}N) in metabolites. Photorespiratory colour scale: O_2 (%)/CO_2 (μmol mol^{-1}). GDC, glycine decarboxylase complex (Ser forming); Ser recycl., Ser utilization (deamination) to synthesize Gly (Ser glyoxylate aminotransferase); GGAT, Glu utilization to synthesize Gly (Glu glyoxylate aminotransferase); GOGAT, Glu production by Gln 2OG aminotransferase; Gly imbal., imbalance between Gly synthesis and consumption (consumption larger than synthesis when >0). In **c**, the solid diagonal is the 1:1 line. In **b**, the region below 10% is shaded and in **a**,**b** the lines represent trends to facilitate the reading. In **a**,**b**, the data shown are associated with two series of three repeats each (means ± s.e.). In **c**, the asterisks stand for significant differences in Gly metabolic imbalance ($P < 0.05$).

Table 1 | Effective stoichiometric coefficient between O_2 fixation by Rubisco and CO_2 production by GDC in photorespiration.

Oxygenation	Gaseous conditions (% O_2/μmol mol^{-1} CO_2)	Average deviation* (%)	Effective stoichiometric coefficient
Near zero	0/380	†	†
Very low	2/380	0	1.99 (±0.02)
Low	21/800	1.1	2.03 (±0.04)
Normal	21/380	2.5	2.05 (±0.03)
High	21/140	3.2‡	2.09 (±0.02)‡
Very high	100/380	4.7	2.08 (±0.06)

Values were computed from isotopic labelling with ^{15}N-Gly. *Excess of Gly production compared with Gly utilization, expressed in %. †In 0% O_2, the photorespiration rate was too low to get a reliable coefficient (values obtained in a wide range: 1.6 to 2.1). ‡Statistically significantly different from 0 (deviation) and 2 (coefficient) at $P < 0.07$.

Gas exchange and online isotopic measurements. Sampling and labelling were carried out in the photosynthetic steady state: after 100 min of stabilization in the desired gaseous condition, isotopic labelling with Gly was started and assimilation was monitored with a Li-Cor 6400 XT to check the photosynthetic steady state. For metabolome kinetics, the photosynthetic steady state was reached (100 min) under ordinary conditions (21% O_2, 380 μmol mol^{-1} CO_2) before changing to new conditions; sampling on the same leaf was carried out 10 min before and 30 min after having changed gaseous conditions and then each 30 min. Online isotope measurements for [^{13}C-1]Gly decarboxylation rates were done as in ref 15. Calculations of the decarboxylation rate were done by mass balance as in ref. 12. See Supplementary Information for further details on gas exchange.

Quantitative ^{15}N-NMR analyses. ^{15}N absolute content in metabolites was analysed using direct ^{15}N observation[16] on leaf perchloric extracts in which an internal standard was added (^{15}N-β-alanine). Within each spectrum, integrals were normalized to that of ^{15}N-β-alanine, and quantitativity for each chemical shift was checked using calibration curves with ^{15}N-labelled amino acids and ^{15}N-β-alanine at different known concentrations. When necessary, a correcting factor was then applied on samples correspondingly (in practice, such corrections factors were not large: they were always very close to 1 (0.95–1.05) showing very small deviation from quantitativity for all observed compounds). Calculation of fluxes using ^{15}N-labelling is described in the Supplementary Information. In these calculations, the subcellular compartmentalization of Gly and Ser[17] and minor alternative metabolic pathways are not taken into account.

Metabolomics and isotope composition. Metabolome profiling was done by gas chromatography mass spectrometry (GCMS) as described in ref. 18. The % ^{15}N was obtained by GCMS computed from m and $m+1$ signals of the nitrogen-containing best-suited fragment[19]. Retention time, quantifying mass and % ^{15}N accuracy were checked by injection of standards. The % ^{13}C in methenyl tetrahydrofolate and *S*-adenosylmethionine were obtained by liquid chromatography mass spectrometry (LCMS) (see Supplementary Information for further LCMS acquisition details).

Received 29 July 2015; accepted 14 December 2015; published 25 January 2016

References

1. Farquhar, G. D. *Phil. Trans. R. Soc. Lond. B* **323,** 357–367 (1989).
2. Zelitch, I. *Proc. Natl Acad. Sci. USA* **70,** 579–584 (1973).
3. Anav, A. *et al. Rev. Geophys.* **53,** 785–818 (2015).
4. Douce, R., Bourguignon, J., Neuburger, M. & Rebeillé, F. *Trends Plant Sci.* **6,** 167–176 (2001).
5. Timm, S. *et al. Plant Cell* **27,** 1968–1984 (2015).
6. Novitskaya, L., Trevanion, S. J., Driscoll, S., Foyer, C. H. & Noctor, G. *Plant Cell Environ.* **25,** 821–835 (2002).
7. Dirks, R. C., Singh, M. & Potter, G. S. *New Phytol.* **196,** 1109–1121 (2012).
8. Von Caemmerer, S. & Farquhar, G. D. *Planta* **153,** 376–387 (1981).
9. Bloom, A. J., Burger, M., Rubio Asensio, J. S. & Cousins, A. B. *Science* **328,** 899–903 (2010).
10. Scheible, W. R., Krapp, A. & Stitt, M. *Plant Cell Environ.* **23,** 1155–1167 (2008).
11. Tcherkez, G. *et al. Plant Cell Environ.* **35,** 2208–2220 (2012).
12. Tcherkez, G. *et al. Proc. Natl Acad. Sci. USA* **105,** 797–802 (2008).

13. Rachmilevitch, S., Cousins, A. B. & Bloom, A. J. *Proc. Natl Acad. Sci. USA* **101,** 11506–11510 (2004).
14. Bloom, A. J., Burger, M., Kimball, B. A. & Pinter, P. J. *Nature Clim. Change* **4,** 477–480 (2014).
15. Tcherkez, G., Cornic, G., Bligny, R., Gout, E. & Ghashghaie, J. *Plant Physiol.* **138,** 1596–1606 (2005).
16. Mesnard, F. & Ratcliffe, R. G. *Phot. Res.* **83,** 163–180 (2005).
17. Krüger, S. *et al. PLoS One* **6,** e17806 (2011).
18. Noctor, G. *et al. Metabolomics* **3,** 161–174 (2007).
19. Tcherkez, G. *et al. Funct. Plant Biol.* **39,** 959–967 (2012).

Acknowledgements

We thank R. Bligny for carrying out analyses associated with preliminary tests for quantitative ^{15}N-NMR, Bruker Biospin for its contribution to find the best NMR quantitative analytical conditions and the Plateforme Métabolisme-Métabolome for access to IRMS, GCMS, NMR and LCMS facilities. This work was supported by the French Agence Nationale de la Recherche via a project Jeunes Chercheurs (under contract JC12-0001-01) and the Australian Research Council via a Future Fellowship (under contract FT140100645).

Author contributions

E.R.A.B.-F., C.A. and G.T. performed experimental work; G.T. and C.A. designed the experiments; A.J.C. performed database searching (metabolomics); G.T. wrote the paper.

Additional information

Supplementary information is available online. Reprints and permissions information is available online at www.nature.com/reprints. Correspondence and requests for materials should be addressed to G.T.

Competing interests

The authors declare no competing financial interests.